

## Characterization of Chars from Steam Pyrolysis of Apricot Pulp

N. Özbay & A. E. Pütün

To cite this article: N. Özbay & A. E. Pütün (2011) Characterization of Chars from Steam Pyrolysis of Apricot Pulp, Energy Sources, Part A: Recovery, Utilization, and Environmental Effects, 33:16, 1504-1513, DOI: [10.1080/15567030903397958](https://doi.org/10.1080/15567030903397958)

To link to this article: <https://doi.org/10.1080/15567030903397958>



Published online: 08 Jun 2011.



Submit your article to this journal [↗](#)



Article views: 138



View related articles [↗](#)



Citing articles: 1 View citing articles [↗](#)

# Characterization of Chars from Steam Pyrolysis of Apricot Pulp

N. ÖZBAY<sup>1</sup> and A. E. PÜTÜN<sup>2</sup>

<sup>1</sup>Department of Process and Chemical Engineering, Bilecik University, Bilecik, Turkey

<sup>2</sup>Department of Chemical Engineering, Anadolu University, Eskisehir, Turkey

**Abstract** *The characterization of apricot pulp char obtained from steam pyrolysis was studied. The char was prepared by pyrolyzing apricot pulp temperatures ranging from 300 to 700°C under steam atmospheres. The chemical composition of char was characterized by Fourier transform infrared spectroscopy. The surface area of the char was measured with the Brunauer–Emmett–Teller method, and surface morphology was obtained with scanning electron microscopy. The char yield in pyrolysis decreased rapidly with an increase in temperature from 39.1% at 300°C to 18.9% at 550°C. The surface area of the char increased with temperature to a maximum of 332 m<sup>2</sup>/g at 550°C. Scanning electron microscopy analysis indicated that the pyrolysis led to the formation of melt, liquid phase, vesicles, precipitates of inorganic salts, and surface etching. Fourier transform infrared spectroscopy studies showed a gradual decrease in the amounts of OH and CH<sub>3</sub> with increasing temperature. Both the H/C and O/C ratios of the char decreased with an increase in temperature.*

**Keywords** apricot pulp, char, characterization, pyrolysis

## 1. Introduction

Pyrolysis of biomass has been a major commercial interest with hopes of producing new fuels, intermediate compounds for the chemical industry, as well as controlling the products produced from obligatory pyrolysis processes. Pyrolysis is one of the primary thermochemical conversion methods to convert biomass into valuable products, namely solid char, liquid, and gas product yields and compositions of which depend on pyrolysis conditions (Bridgewater and Grassi, 1991). The properties of the char obtained after biomass devolatilization have a direct influence on the subsequent char oxidation step, since the amount and type of pores determine the gas accessibility to the active surface sites (Liu et al., 2000; Chan et al., 1999; Arenillas et al., 2003).

Textural properties of char are decisively affected by not only the properties of the parent material, but also by the operating conditions used, mainly the heating rate, the maximum temperature experienced, and the residence time at this temperature. This is because these variables, together with biomass properties, influence the amount and nature of the volatiles produced during pyrolysis, as well as their rate of release. These factors also determine both the macroscopic morphology and the microscopic porosity of the resultant char (Guerrero et al., 2005).

Address correspondence to Nurgül Özbay, Department of Process and Chemical Engineering, Bilecik University, Bilecik, Turkey. E-mail: nozbay@anadolu.edu.tr

Turkey is the biggest apricot producer in the world with a production of 538,000 tons (134,500 tons pit) which constitutes 20.15% of world production. There are 13,350,000 apricot trees, of which approximately 10,710,000 are fruit-bearing and 2,640,000 are nonfruit-bearing. Most of apricots are produced in the Malatya region in Turkey. This region has a 60% share of fresh apricot production and an 80% share of dried apricot production in Turkey (Gezer et al., 2002).

In this article, the char was prepared by pyrolyzing apricot pulp (AP) temperatures ranging from 300 to 700°C under steam atmosphere. The chemical composition of the char was characterized with Fourier transform infrared spectroscopy (FTIR). The elemental composition and surface area were also determined. The surface morphology of char was studied by scanning electron microscopy (SEM).

## 2. Experimental

### 2.1. Raw Material

AP used in this work was obtained from fruit juice factories around Bursa, which is located in Western Anatolia. Air-dried pulps were ground to obtain a uniform material of an average particle size (1.122 mm). The average bulk density of this raw material was found to be 411.5 kg/m<sup>3</sup>. The proximate analyses of the raw material having an average particle size were performed according to ASTM procedures, and the moisture, ash, and volatile matter contents were found to be 10.3, 4.7, and 71.95 wt%, respectively. The rest is calculated to be the percentage of fixed carbon at 13.04. AP contains 23.58% cellulose and 3.76% acid-insoluble lignin. Hexane solubles of AP correspond to oil content that was 1.11 wt%.

The elemental analysis of AP was performed using Carlo Erba EA 1108-type equipment for C, H, and N. Oxygen was determined by the difference. Elemental analysis showed that it consisted of 51.4% carbon, 5.7% hydrogen, 2.5% nitrogen, and 40.2% oxygen.

FTIR spectrum of AP was recorded to have further information on the chemical structure of the raw material in the near infrared region, 400–4,000 cm by preparing KBr pellet.

The thermal behavior of AP to 900°C was studied using a Linseis Thermowaage L 81 thermogravimetric analyzer.

### 2.2. Pyrolysis Procedure

The pyrolysis of the air-dried AP was carried out in a fixed-bed reactor steam atmosphere and experimental details have been given elsewhere (Ozbay et al., 2006).

For the pyrolysis experiments, a 10-g sample of pulp was placed into the reactor and pyrolyzed under water vapor atmosphere with a flow rate of 2.5 cm<sup>3</sup> min<sup>-1</sup> and a heating rate of 5°C min<sup>-1</sup> to the final temperature of 300, 400, 450, 500, 550, and 700°C and held for either a minimum of 30 min or until no further significant release of gas was observed.

After reaching the final pyrolysis temperature, the reactor was set to cool to room temperature. Pyrolysis product yields were determined gravimetrically by weighing the three products. The liquid phase was collected in cold traps maintained at about 0°C using salty ice. The liquid phase consisted of aqueous and oil phases, which were separated and weighed. Solid product (char) was removed from the reactor and weighed. The flow

of gas released was controlled using a soap film for the duration of experiments. The gas yield was calculated by the difference.

### 2.3. Char Characterization

Proximate analysis was applied to the chars obtained at six different pyrolysis temperatures to figure out the moisture, ash, and volatile contents according to ASTM methods. The elemental analyses of the chars were performed with a Carlo Erba 1108 elemental analyzer.

The FTIR spectra were recorded in the transmission mode between 4,000 and 400  $\text{cm}^{-1}$  using a Bruker Tensor 27 model Fourier transform infrared spectrometer.

The surface area of the chars was measured in automated volumetric gas adsorption apparatus (Quantochrome Co.) using nitrogen as an adsorbate at 77 K. The surface characteristics of the chars were analyzed using a scanning electronic microscope Jeol Camscan. Obtained chars were mounted on an aluminum stub using carbon film and were coated with a thin layer of gold and palladium using Agar Sputter Coater.

## 3. Result and Discussion

### 3.1. FTIR Spectrum of AP

For AP, the FTIR spectroscopy provides information on chemical structure of the material as follows. Figure 1 shows that AP contains a number of atomic groups and structures (OH,  $\text{CH}_2$ ,  $\text{C}=\text{O}$ ,  $\text{C}-\text{O}-\text{C}$ , and so on). The position and shape of the band  $3,343 \text{ cm}^{-1}$  are compatible with the involvement of the hydroxyl groups in hydrogen bonding. Otherwise, the band should be located at significantly higher wavenumbers and it should be much sharper. For free OH groups, the band is located at  $\sim 3,625 \text{ cm}^{-1}$  for alcohols,  $3,605 \text{ cm}^{-1}$  for broader toward lower wavenumbers suggests that, though phenols and  $3,530 \text{ cm}^{-1}$  for carboxylic acids (Gomez-Serrano et al., 1999).

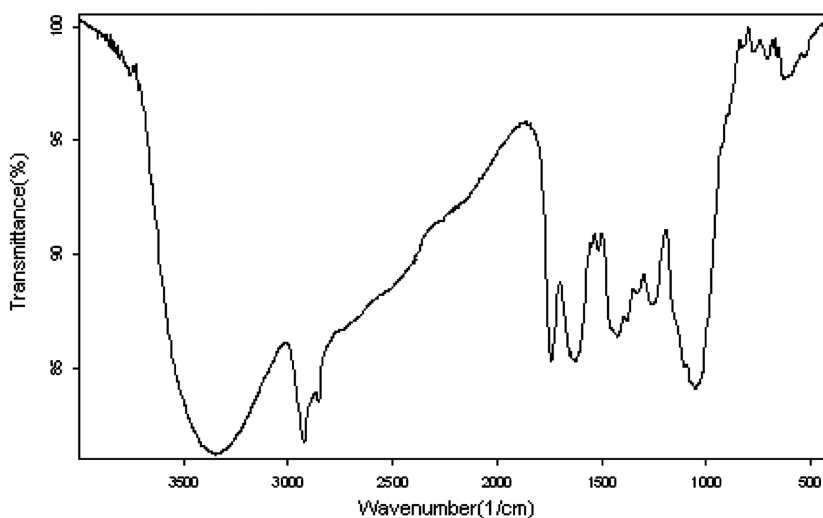


Figure 1. FTIR spectrum of apricot pulp (AP).

The band at  $2,921\text{ cm}^{-1}$  is connected with  $\nu_{as}$  and  $\nu_s$  vibration modes of methyl and methylene groups. The characteristic absorption of the methyl group near  $1,377\text{ cm}^{-1}$  is diagnostically useful, since it has been used in methyl group estimation. In addition, the  $1,400\text{ cm}^{-1}$  region gives an idea on relative abundance  $\text{CH}_2$  and  $\text{CH}_3$  groupings. For organic compounds, the band  $1,460$  is frequently stronger than the band  $1,377\text{ cm}^{-1}$ . Other bending vibration modes for the  $\text{CH}_2$  groups (i.e., rocking, wagging, and twisting) give rise to bands at lower frequencies. These bands are usually weak; therefore, they have little practical utility (Gomez-Serrano et al., 1996).

The shoulder at  $1,626\text{ cm}^{-1}$  in the spectrum of AP is attributable to  $\nu(\text{C}=\text{C})$  vibrations in terminal olefinic  $\text{C}=\text{C}$  bonds. In connection with this spectral region between  $1,700$  and  $1,600\text{ cm}^{-1}$ , there is overlapping of bands and, as a result, the absorption maximum may shift toward lower wavenumbers (Gomez-Serrano et al., 1999). Of the aromatic skeletal stretching bands, only three at  $1,595$ ,  $1,510$ , and  $1,460\text{ cm}^{-1}$ , are readily visible in the spectrum. Note that the band at  $1,510\text{ cm}^{-1}$  is stronger than the band at  $1,595$ , as usual for aromatic rings. The  $1,460\text{ cm}^{-1}$  peak overlaps with the  $\text{CH}_3$  and  $\text{CH}_2$  band. The single band at  $775\text{ cm}^{-1}$  is characteristic of *p*-disubstituted phenyl groups that possess two adjacent hydrogen atoms.

### 3.2. Thermal Analysis

Figure 2 shows the thermo gravimetric (TG) and derivative thermo gravimetric (DTG) curves of AP obtained from room temperature to  $850^\circ\text{C}$  with a heating rate of  $10^\circ\text{C}/\text{min}$ . Biomass is typically composed of cellulose, hemicelluloses, and lignin. Four weight loss steps can be identified in DTG curves. The first weight loss occurs between  $50$  and  $150^\circ\text{C}$ . The second step between  $200$  and  $260^\circ\text{C}$ , with the maximum weight loss rate at  $203^\circ\text{C}$ , is attributable to degradation of hemicelluloses. The third step, between  $300$  and  $350^\circ\text{C}$ , with the maximum weight loss rate at  $314^\circ\text{C}$ , would correspond to thermal degradation of cellulose. The last weight loss step, ascribable to lignin degradation, appears between ca  $150$  and  $480^\circ\text{C}$ . The occurrence and assignment to hemicelluloses, cellulose, and lignin of the different weight loss steps, are well documented in the literature for pyrolysis of other types of lignocellulosic materials (Orfao et al., 1999; Li et al., 2004).

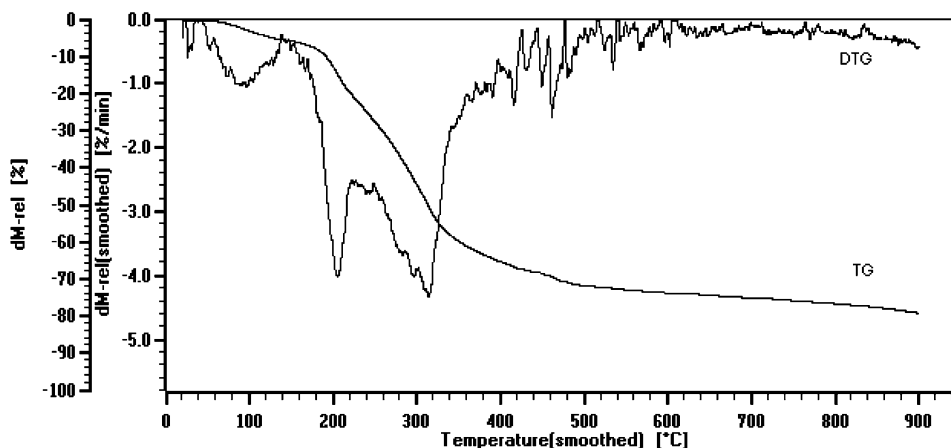
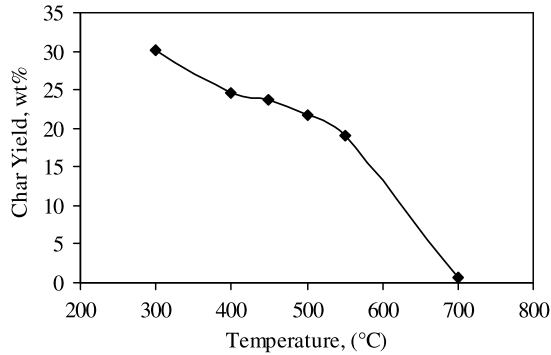


Figure 2. DTG and TG curves for AP.



**Figure 3.** Effect of temperature on char yield.

### 3.3. Char Yield

Figure 3 shows the effect of temperature on char yield. The term “char” is used to represent the solid residue that remained after pyrolysis and consisted of organic material with decomposition varying from barely pyrolyzed biomass (AP) at low temperatures to a highly carbonized material at high temperatures. The char also included any coke that might have been formed by the reactions among the volatile components (Sharma et al., 2000). In steam pyrolysis experiments, the yield of char decreased with an increase in temperature from 39.1% at 300°C to 18.9% at 550°C. Above 550°C, the char yield became negligibly small due to rapid oxidation of AP and char in the presence of oxygen.

### 3.4. Char Characterization

**3.4.1. Elemental Analysis.** Figure 4 shows the results for moisture, ash, and volatile matter content of the chars obtained at six different temperatures. As the temperature is raised, there is a rise in ash content and fixed carbon percentage and there is a decrease

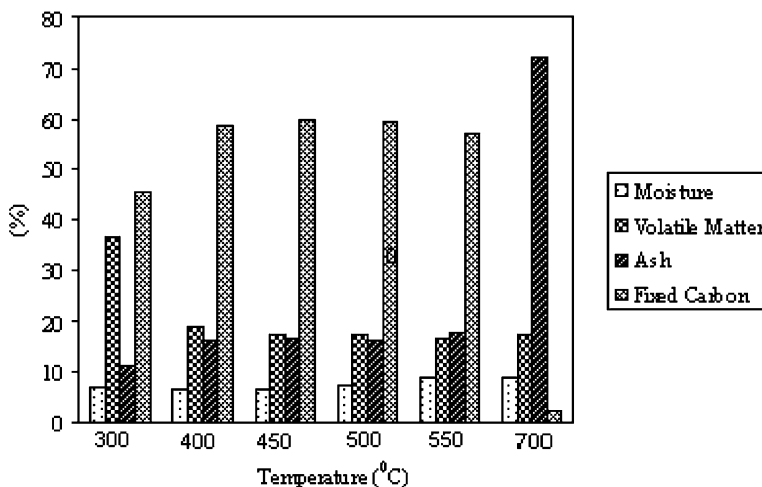


**Figure 4.** Proximate analyses of chars at different temperatures.

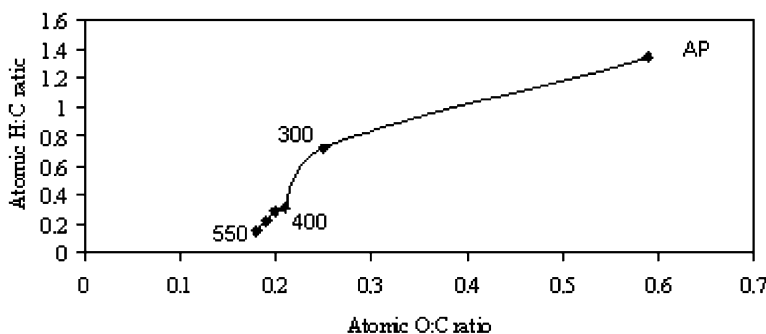


**Figure 5.** Van Krevelen diagram for AP and its chars obtained at different temperatures.

in volatile matter content due to gasification reactions occurring at higher pyrolysis temperatures. Consequently, higher temperature yields charcoals of greater quality.

The elemental composition of the various chars is presented in Figure 5. The compositions are given as a plot of hydrogen/carbon ratio (H/C) against the (O/C) in the form of the Van Krevelen diagram (Sharma and Hajaligol, 2003). For the pyrolysis chars, the H/C ratio decreased continuously with an increase in temperature from ca 0.72 for the char at 300°C to 0.15 for the char at 550°C. The O/C ratio also decreased, from 0.25–0.18 in the same temperature range. This indicates a loss of hydrogen and oxygen and a gradual enrichment of char with carbon.

**3.4.2. Surface Area.** The surface area of char is important because, like other physicochemical characteristics, it may strongly affect the reactivity and combustion behavior of the char. The surface area was generally low with  $\sim 1$  m<sup>2</sup>/g at 300–450°C, but the area increased dramatically to 332 m<sup>2</sup>/g for char prepared at 550°C. Thus, there is an optimum temperature for the maximum surface area. The omitted surface area values suggested that the pores might be virtually closed at low temperatures, thus preventing any access to adsorbing gas. SEM reveals large macropores that contribute only little to the surface area. The high surface area at 550°C was probably due to the micropores because the micropore samples with open pores are expected to have high surface areas (Guerrero et al., 2005; Sharma and Hajaligol, 2003; Sharma et al., 2001).

**3.4.3. FTIR Analysis.** For the structural analysis, chars obtained at six different temperatures were conducted to FTIR. The FTIR spectra for chars are presented in Figure 6. When compared to FTIR spectra of AP with the char obtained from AP at 300–700°C, the major changes were reported in the chemical structure of the material. Thus, the presence of OH, CH<sub>2</sub>, and C=O groups and of olefinic structure undergo a drastic reduction in the char.

The asymmetric and symmetric vibration modes of methyl and methylene groups appeared to be 2,918 and 2,850 cm<sup>-1</sup> in chars, and intensity decreased as the temperature increased from 300 to 700°C and this band completely disappeared above 500°C.

The shoulder at  $\sim 1,550$  cm<sup>-1</sup> is attributable to in-plane skeletal vibrations in aromatic rings. The variations in aromatic CH wags in the 900–700 region were used to study the changes in aromatic structures. The substitution bands appear at 875, 837, and 757 cm<sup>-1</sup>, which are band positions compatible with  $\gamma$ (C–H) vibrations in a system having

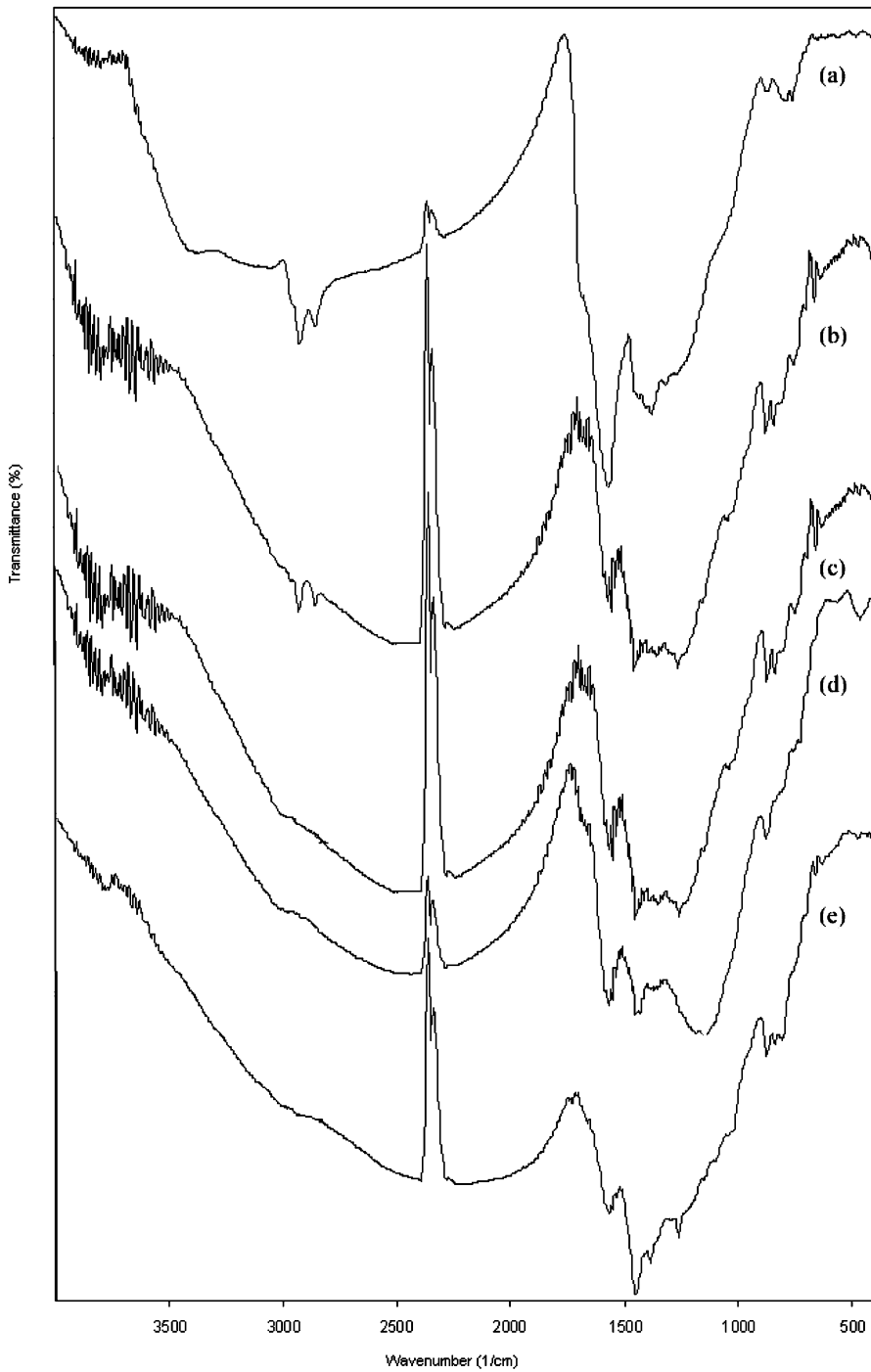


**Figure 6.** FT-IR spectra of chars obtained at different temperatures: (a) 300°C, (b) 400°C, (c) 500°C, (d) 550°C, (e) 700°C.

3, 4, and 5 adjacent hydrogen atoms, such as substituted naphthalene, anthracene, or phenanthrenes. The band decreased at high temperatures due to the aromatic ring mode.

The shoulder at  $1,240\text{ cm}^{-1}$  and a band at  $1,110\text{ cm}^{-1}$  in the spectrum of the aforementioned carbonized assigned to  $\gamma(\text{C-O})$  vibrations in ether structures to  $\nu(\text{C-O})$  absorption may also contribute a low concentration of phenolic groups, in accordance with the slight absorption of infrared radiations in the spectral region  $\nu(\text{O-H})$  vibration (Sharma et al., 2004; Silverstein et al., 1974; Gomez-Serrano et al., 2002).

**3.4.4. SEM Analysis.** The results of SEM analysis of chars obtained at four different temperatures are shown in Figure 7. Analysis of the char at  $300^\circ\text{C}$  showed that there appeared to be closed vesicles within vesicles. The presence of vesicles indicates that volatile components were formed and released, and that the vesicles occurred through plastic deformation, a melt phase of cellular components (Baliga et al., 2003). The increase in pyrolysis temperature leads to formation of pores on the surface. At  $400^\circ\text{C}$ , both open and closed vesicles were present. Open pores might have been formed by the breaking and remelting of some of the bubbles.

At  $550^\circ\text{C}$ , large bubbles that were formed in the melt appeared to break rapidly, probably due to a large increase in the rate of formation of volatile products. Equant-shaped particles may be the result of secondary product formation from the precipitation of volatile gases. The micro porous structure of the char is readily visible as shown in Figure 7d. Closed vesicles at the beginning of the canals were exploded and the volatiles inside the canals moved away as gaseous products during pyrolysis. Furthermore, it

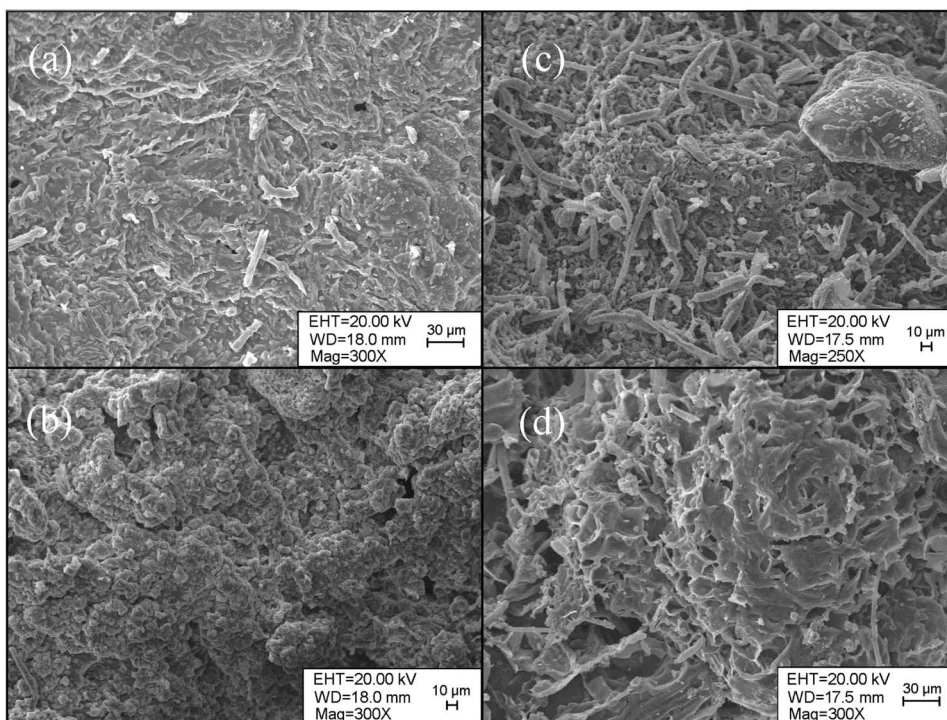


**Figure 7.** Scanning electron micrographs of AP char obtained at different pyrolysis temperatures: (a)  $300^\circ\text{C}$ , (b)  $400^\circ\text{C}$ , (c)  $550^\circ\text{C}$ , (d)  $700^\circ\text{C}$ .

should be noted that the emptied canals have a cylindrical regular shape with a diameter of 6.5  $\mu\text{m}$ .

#### 4. Conclusion

Fruit juice factories' waste AP was taken as the biomass sample for pyrolysis experiments performed in a fixed-bed static reactor.

The results in this study showed that both the yield and characteristics of chars from AP were dependent on the pyrolysis temperatures. The yield of char decreased with an increase in temperature from 39.1% at 300°C to 18.9% at 550°C. Above 550°C, the char yield became negligibly small due to rapid oxidation of AP and char in the presence of oxygen. The surface area was generally low with  $\sim 1 \text{ m}^2/\text{g}$  at 300–450°C, but maximum surface area of the char occurred at 550°C and appeared to be associated with the completion of the solidification stage within the char. SEM reveals mainly large macropores that contribute little to the surface area. Besides, as a result of the softening, melting, and carbonization, pores in the chars might be partially blocked. This would prevent the access of the adsorbing gas to the pores and lead to low surface area. Both H/C and O/C of the char decreased with an increase in temperature. This indicates a loss of hydrogen and oxygen and a gradual enrichment of char with carbon. The chars became increasingly more aromatic with the increase in temperature.

#### References

- Arenillas, A., Rubiera, F., Parra, J. B., and Piskorz, J. J. 2003. Coal structure and reactivity changes induced by chemical demineralisation. *Fuel Process. Technol.* 77/78:103.
- Bridgewater, A. V., and Grassi, G. 1991. *Biomass Pyrolysis Liquids Upgrading and Utilization*. England: Elsevier Applied Science.
- Chan, M. L., Jones, J. M., Pourkashanian, M., and Williams, A. 1999. The oxidative reactivity of coal chars in relation to their structure. *Fuel* 78:1539–1552.
- Gezer, I., Haciseferogullari, H., and Demir, F. 2002. Some physical properties of Hacıhalioğlu apricot pit and its kernel. *J. Food Eng.* 56:49–57.
- Gomez-Serrano, V., Alvarez, P. M., Jaramillo, J., and Beltran, F. J. 2002. Formation of oxygen complexes by ozonation of carbonaceous materials prepared from cherry stones, I. Thermal effects. *Carbon* 40:513–522.
- Gomez-Serrano, V., Piriz-Almeida, F., Duran-Valle, C. J., and Pastor-Villegas, J. 1999. Formation of oxygen structures by air activation. A study by FT-IR spectroscopy. *Carbon* 37:1517–1528.
- Gomez-Serrano, V. G., Villegas, J. P., Florindo, A. P., Vale, C. D., and Valenzuela-Calohorro, C. 1996. FT-IR study of rockrose and of char and activated carbon. *J. Anal. Appl. Pyrol.* 36:71–80.
- Guerrero, M., Ruiz, M. P., Alzueta, M. U., Bilbao, R., and Millera, A. 2005. Pyrolysis of eucalyptus at different heating rates: Studies of char characterization and oxidative reactivity. *J. Anal. Appl. Pyrol.* 74:307–314.
- Li, S., Xu, S., Liu, S., Yang, C., and Lu, Q. 2004. Fast pyrolysis of biomass in free-fall reactor for hydrogen-rich gas. *Fuel Process. Technol.* 85:1201–1211.
- Liu, G., Benyon, P., Benfell, K. E., Bryant, G. W., Tate, A. G., Boyd, R. K., Harris, D. J., and Wall, T. F. 2000. The porous structure of bituminous coal chars and its influence on combustion and gasification under chemically controlled conditions. *Fuel* 79:617–626.
- Orfao, J. M., Antune, F. J., and Figueiredo, J. L. 1999. Pyrolysis kinetics of lignocellulosic materials—three independent reactions models. *Fuel* 78:349–358.
- Ozbay, N., Uzun, B. B., Apaydin-Varol, E., and Putun, A. E. 2006. Comparative analysis of pyrolysis oils and its subfractions under different atmospheric conditions. *Fuel Process. Technol.* 87:1013–1019.

- Sharma, R. K., Wooten, J. B., Baliga, V. L., Lin, X. C., Chan, W. G., and Hajaligol, M. R. 2004. Characterization of char from pyrolysis of lignin. *Energy & Fuels* 14:1083–1093.
- Sharma, R. K., and Hajaligol, M. R. 2003. Effect of pyrolysis conditions on the formation of polycyclic aromatic hydrocarbons (PAHs) from polyphenolic compounds. *J. Anal. Appl. Pyrol.* 66:123–144.
- Sharma, R. K., Wooten, J. B., Baliga, V., and Hajaligol, M. R. 2001. Characterization of chars from biomass-derived materials: Pectin chars. *Fuel* 80:1825–1836.
- Sharma, R. K., Hajaligol, M. R., Mortoglio Smith, P. A., Wooten, J. B., and Baliga, V. 2000. Characterization of char from pyrolysis of chlorogenic acid. *Energy & Fuels* 14:1083–1093.
- Silverstein, R. M., Bassler, G. C., and Morrill, T. C. 1974. *Spectrometric Identification of Organic Compounds*, 3rd Ed. New York: Wiley, p. 85.